Complete Characterization of Electrostatically-Actuated Beams including Effects of Multiple Discontinuities and Buckling

E. K. Chan, K. Garikipati, and R. W. Dutton
CISX 305, Center for Integrated Systems
Stanford University, Stanford, CA 94305-4075
Email: edward_chan@alumni.stanford.org

ABSTRACT

The entire process of calibrating an electromechanical simulator – identifying relevant parameters, designing and measuring test structures, extracting parameters using detailed electromechanical simulations, and extrapolating the behavior of an actual device – is presented. The simulation model for electrostatically-actuated beams is calibrated to a wide range of electrical and optical test structure measurements and is then used to predict the behavior of more complex dual-bias-electrode structures. Various mechanical discontinuities, and post-buckled pull-in behavior are addressed explicitly. Arbitrary fitting coefficients that limit generality are avoided. The well-characterized behavior of the dual-electrode structures can serve as verification test cases for evaluating coupled electromechanical simulators.
Keywords: *calibration, electromechanical, simulation*

INTRODUCTION

Computer simulation tools need to be thoroughly calibrated to particular fabrication processes in order to produce useful and accurate results. The calibration steps consist of identifying relevant simulation model parameters, designing suitable test structures, extracting parameters using detailed yet fast electromechanical simulations, and finally extrapolating the behavior of an actual complex device. Electrostatically-actuated beams fabricated in the POLY1 layer of MUMPs [2] are considered here. Caution must be exercised whenever simulating different actuation mechanisms or devices with dimensions beyond the range of the calibration. Uniformity of material properties cannot always be extrapolated.

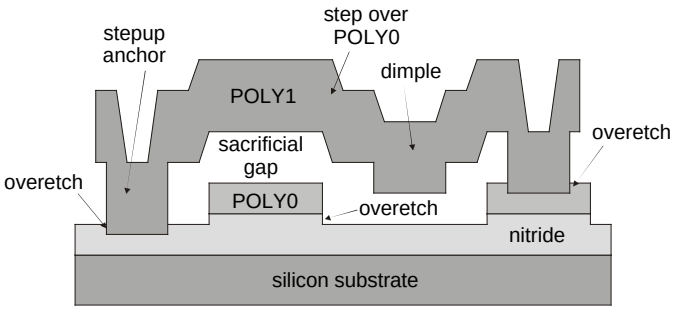

Fig. 1. *Profile of typical electrostatically-actuated structure showing discontinuities and effects of overetch.*

This simulation-based model consisting of geometrical and material property information precludes the need for rather ad hoc parametric adjustments and simplifying assumptions [3][5]. The model is calibrated to both optical and electrical measurements thus increasing confidence in the extracted parameters. The MUMPs system of materials is first described, highlighting the observed variations among beams of different width, the effects of overetch, and the influences of gold pads. Calibration of flat beams to pull-in voltages (V_{pi}) and buckling amplitudes is explained next. The calibration steps are then repeated for beams with steps over underlying POLY0 pads, and beams with dimples. Finally, the well-characterized Abaqus simulation model is extended to predict the behavior of dual-bias-electrode structures. The extrapolation is very good, verifying the accuracy of the calibration methodology.

MATERIALS SYSTEM

Measurements were made on a single die on the MUMPs27 run unless otherwise noted. The die was supercritically dried after a 2.5 minute HF release to obtain long freestanding beams. Rather than trying to extract parameters in light of run-to-run or even die-to-die variations, the goal of this paper is to come up with very accurate geometric and material properties, and hence to validate a parameter extraction methodology and its underlying coupled electromechanical simulation model.

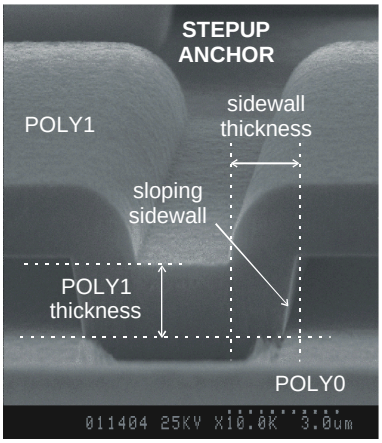

Fig. 2. *SEM of stepup anchor showing thickness measurement site, and sidewall geometry.*

Fig. 1 of an electrostatically-actuated beam shows steps/discontinuities and overetches. The geometric properties of interest are the thicknesses of layers, and shapes of the stepup anchors and other steps. The electrical thickness of the nitride was determined from capacitance measurements. All thicknesses and height measurements were made using a Zygo NewView 200 interferometer. The thickness of the POLY1 layer was measured at the base of a stepup anchor deposited on

POLY0 as shown in the SEM of Fig. 2. The overetch of about 0.03μm of the underlying POLY0 pad during the ANCHOR1 etch causes the measured thickness to be slightly less than the actual thickness. This discrepancy is offset in part by the overetch of the underside of an actual freestanding beam during the HF release, and by surface roughness which adds to optical thickness measurements but not to structural rigidity. All thicknesses used in subsequent simulations are shown in Table 1.

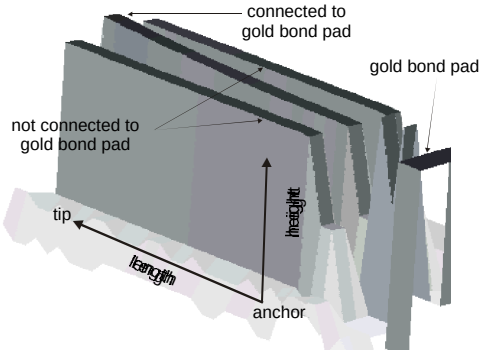

Fig. 3. *Interferometric image of three unloaded, freestanding POLY1 cantilevers with similar designs except that the center one is connected to a gold bond pad. The center cantilever curls up more. Interferometric images only show top surfaces therefore the sacrificial gap is not displayed.*

The sacrificial gap is determined by subtracting the thickness of the POLY1 layer from the height of an unreleased POLY1-plus-PSG stack deposited on POLY0. POLY0 layers connected to gold bonding pads are about 0.01μm thinner, and have rougher surfaces and hence lower reflectivity than isolated POLY0 layers. This might be due to an electrochemical potential set up by the gold pads that increases the etch rate of the POLY0 layer during the sacrificial HF etch. The influence of a gold pad depends on the amount of exposed surface area of the polysilicon part that it is connected to. This slight etching of the POLY0 layer causes the sacrificial gap in between the nitride and POLY1 to be about 0.01μm less than the gap between the POLY0 and POLY1. Another effect of gold is visible in Fig. 3 which shows that the cantilever connected to a gold pad curls up more than the other two cantilevers.

The behavior of the beams also shows a dependence on their widths. Fig. 4 shows cantilever beams, all without connections to gold, that curl down with different radii of curvature with the exception of the anomalous 10μm-wide beam which actually curls up. In addition, each of the beams exhibits variations in height along its width as shown in the cross-sectional profile. The top surfaces of the narrower beams (less than 50μm wide) are rounded. It is difficult to determine if this roundedness is due to bending or to uneven etching of the surface. The wider beams show saddle-like height variations with rounded ridges near each edge. It is possible that the two ridges coalesced into one mound in the case of the narrower beams. Since the source of such widthwise variations is unclear, only 30μm-wide beams are used for the calibration to minimize the effects of non-ideal cross-sections while avoiding the saddle-like height variations.

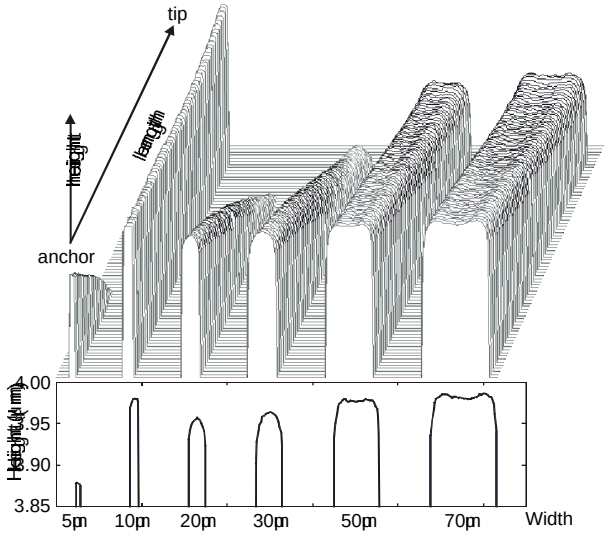

Fig. 4. *Interferometric image of the unloaded deflection of released cantilevers of various widths fabricated in MUMPs 25.*

Table 1: Simulation Parameters

Measured Thicknesses (μm)	
POLY0 (with gold)	0.53
POLY0 (without gold)	0.54
POLY1	1.99
Sacrificial PSG	2.16
Nitride (electrical)	0.074
Stepup sidewall	1.80

Extracted Properties	
Initial biaxial stress	7.8 MPa
Young's modulus	135 GPa

CALIBRATION TO FLAT BEAMS

For the best match to simulations, the beams, flat except for the anchor stepups, were designed to be essentially two-dimensional without POLY1 enclosure lips around the anchors [1]. The 2D simulation model in Abaqus™ incorporates overetch, sloping sidewalls and conformal deposition.

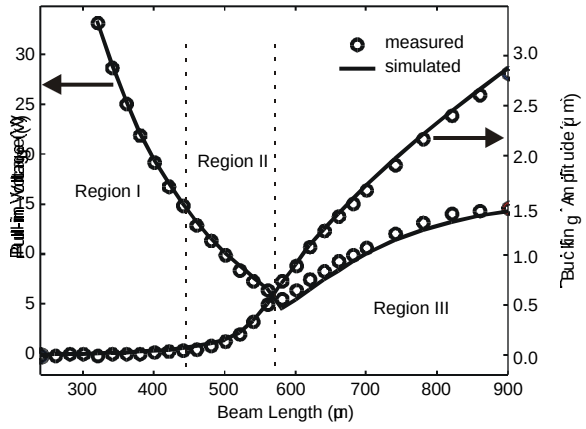

Fig. 5. *Pull-in voltages and buckling amplitude of flat beams as functions of beam length. Three regions of pull-in behavior are demarcated.*

The beams tend to deform to relieve some initial as-deposited compressive stress. The amplitude of the deflection depends on initial strain, beam length, thickness and boundary

conditions. In contrast to the ideal case where deflection occurs only beyond a threshold buckling beam length, beams with stepup anchors deform even at shorter lengths as shown in Fig 5. The strain parameter can be extracted by fitting Abaqus simulations to the measured buckling amplitudes for various beams. The excellent fit indicates that the other parameters critical to buckling amplitude are as determined from interferometric measurements and SEMs. Measurements of beams with backfilled stepup anchors [7] show that the pressure due to encapsulated PSG in such anchors causes the beams to always deflect downwards instead of upwards, and with larger amplitudes as shown in Fig. 6.

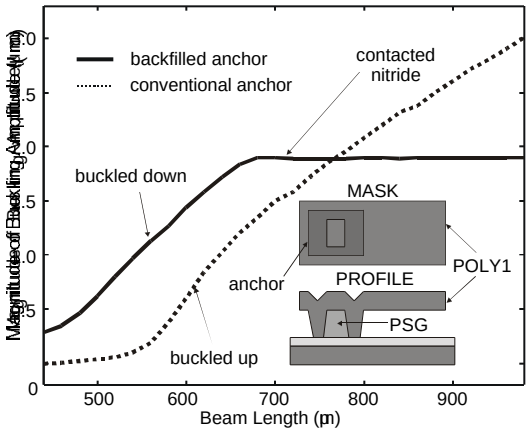

Fig. 6. *Measured magnitude of buckling amplitude for beams with backfilled anchors compared to beams with conventional anchors. Beams are from MUMPs 25 run.*

Young's modulus can be extracted by fitting simulation results to V_{pi} measurements [3]. An HP 4275A capacitance-voltage (CV) meter was used to apply a bias voltage and to sense the abrupt increase in capacitance at pull-in. The simulation fit is good with the kink at 580μm captured accurately as shown in Fig. 5 although the simulated voltages in Region III are slightly lower than those measured. The three types of pull-in behavior corresponding to the regions in Fig. 5 are shown in Fig. 7. A short beam in Region I will deflect continuously with increasing voltage until the gap decreases to about 1.0μm then snap down to the nitride dielectric. A longer beam in Region II that has an initial buckling displacement deflects continuously then snaps down to a stable state below the zero-displacement position. From

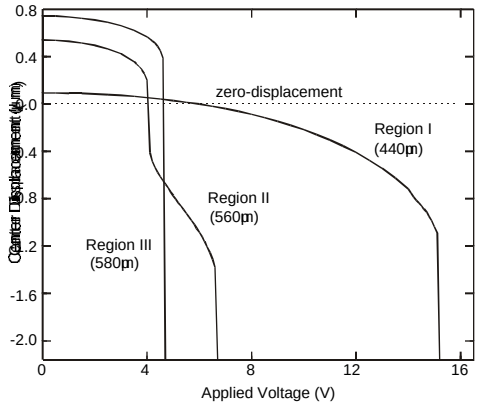

Fig. 7. *Three different types of pull-in behavior.*

there, it continues to deflect with increasing voltage before finally snapping down again, this time contacting the nitride. This two-step pull-down phenomenon does not occur for longer beams in Region III because there is no stable state below zero-displacement so the beams snap down all the way to the nitride. In contrast to beams in the first two regions, beams exhibiting this third type of behavior have V_{pi}'s that increase with beam length because the buckling amplitude and hence the effective gap increases. Therefore, the V_{pi}'s of these post-buckled beams are more sensitive to initial stress than the V_{pi}'s of shorter beams. Table 1 shows extracted properties.

MULTIPLE DISCONTINUITIES

Beams fabricated out of conformal polysilicon can have dimples, and steps over underlying POLY0. Dimple depth and POLY0 thickness were measured optically then included in the

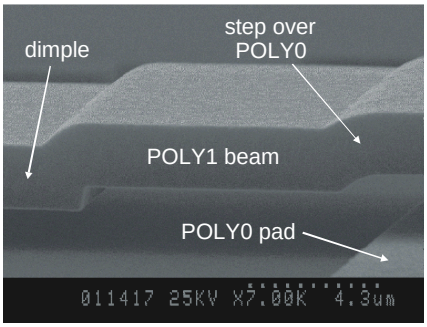

Fig. 8. *SEM of step over POLY0 and step into dimple.*

Abaqus model using the SEM of Fig. 8 as a guide to the actual shape of the discontinuities. The inset in Fig. 9 shows test structures designed to examine the effects of these discontinuities. Once again, the V_{pi}'s and buckling amplitudes of beams of various lengths were measured. The beams over POLY0 behave quite similarly to flat beams as shown in Fig. 9. The transition in buckling amplitudes from the pre-buckled to the post-buckled states is more gradual and begins earlier due to the increased compliance at the boundaries. The amplitudes are also slightly smaller. On the other hand, beams with dimples

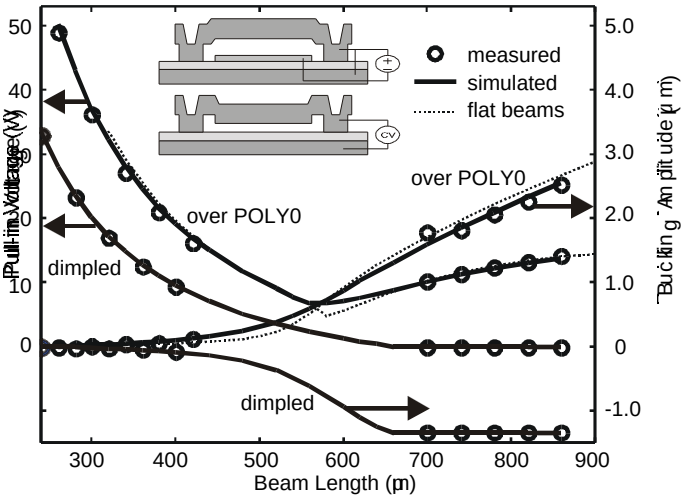

Fig. 9. *Pull-in voltages and buckling amplitude as functions of beam length for beams over POLY0 and beams with dimples. Values for flat beams are in dotted lines.*

buckle downwards systematically instead of upwards. Therefore, the post-buckled V_{pi}'s do not rise with beam length but instead go to zero once the beams buckle into contact with the nitride. The simulation fits are good indicating that the geometrical model is valid.

DUAL-BIAS-ELECTRODE STRUCTURES

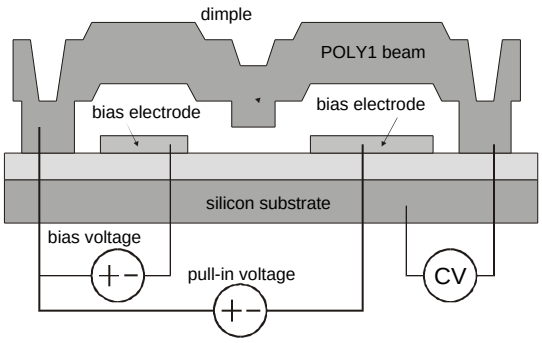

Fig. 10. *Profile of dual-bias-electrode structure.*

The simulation model characterized in the previous sections is now used to predict the behavior of more complex dual-bias-electrode structures shown in Fig. 10. The measurements of Fig. 11 are of V_{pi} at one electrode as a function of bias voltages (V_{bias}) applied to the other electrode for three different devices. The devices were designed such that pull-in is still abrupt despite the leveraging action. By having two bias electrodes, multiple precise pull-in voltage measurements can be made on a single device. The dimple at the center of the beam prevents conductor-to-conductor contact. Dielectric charging [1] should not affect the behavior of the system. The V_{pi} vs. V_{bias} curves for the devices with left and right electrodes of equal length are symmetric about the $V_{pi} = V_{bias}$ line. By swapping the bias and pull-in connections, the integrity of the devices can be verified by checking for symmetry.

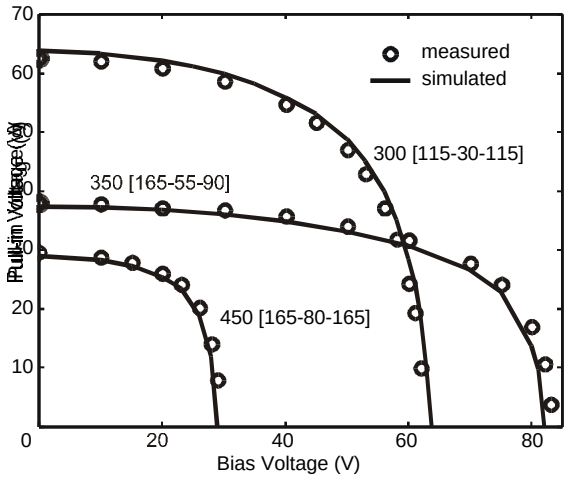

Fig. 11. *Pull-in voltage as a function of bias voltage for three dual-bias-electrode structures. The first number in the label is the beam length. In the brackets are the lengths of the pull-in electrode, dimple, and bias electrode.*

The extrapolated behavior matches the measurements well. For curves such as these with some segments that are primarily vertical, error norms should be calculated along the directions normal to the curves rather than simply taking the differences between the measured and simulated V_{pi}'s at a particular bias. Using this normal-direction error metric, the simulations match the measured values to within 3%. It has thus been demonstrated that the model parameters in Table 1 along with the measurement data in Fig. 11 can be used as verification test cases to evaluate the accuracy of coupled electromechanical simulators.

CONCLUSIONS

A comprehensive methodology to calibrate a simulation model to the MUMPs process of MCNC has been presented. The limits of the calibration procedure due to width-dependent variations and the effects of gold pads were discussed. The extrapolations of the simulation model to more complex devices were excellent demonstrating the viability of the dual-bias-electrode structures to serve as canonical benchmarks for coupled electromechanical simulators.

The authors would like to thank B. K. Eplett for assistance with the SEMs. This work was supported by the DARPA Composite CAD program contract #F30602-96-2-0308-P001.

REFERENCES

[1] E. K. Chan et. al., "Characterization of contact electromechanics through capacitance-voltage measurements and simulations," to appear in *JMEMS*, Mar/Jun 1999.

[2] D. A. Koester et. al., *SmartMUMPs Design Handbook including MUMPs Introduction and Design Rules* (rev. 4), MCNC, Jul 1996.

[3] R. K. Gupta, "Electrostatic pull-in test structure design for in-situ mechanical property measurements of microelectromechanical systems (MEMS)," Ph.D. thesis, MIT, USA, Jun 1997.

[4] J. C. Marshall et. al., "Analysis of fixed-fixed beam test structures," Proceedings of *SPIE* vol. 2880, pp. 46-55, Oct 1996.

[5] W. Fang et. al., "Post-buckling of micromachined beams," *Journal of Micromechanics and Microengineering*, vol. 4 no. 3, pp. 116-122, Sep 1994.

[6] N. M. Wilson et. al., "Utilizing existing TCAD simulation tools to create solid models for the simulation-based design of MEMS devices," *ASME IMECE*, DSC-Vol. 66, pp. 565-570, Nov 1998.

[7] J. J.-Y. Gill et. al., "Elimination of extra spring effect at the stepup anchor of surface micromachined structure," *JMEMS*, vol. 7 no. 1, pp. 114-121, Mar 1998